CRREL REPORT 93-21

Growth Condition of an Ice Layer in Freezing Soils Under Applied Loads

I. Experiment

Kazuo Takeda and Yoshisuke Nakano

November 1993

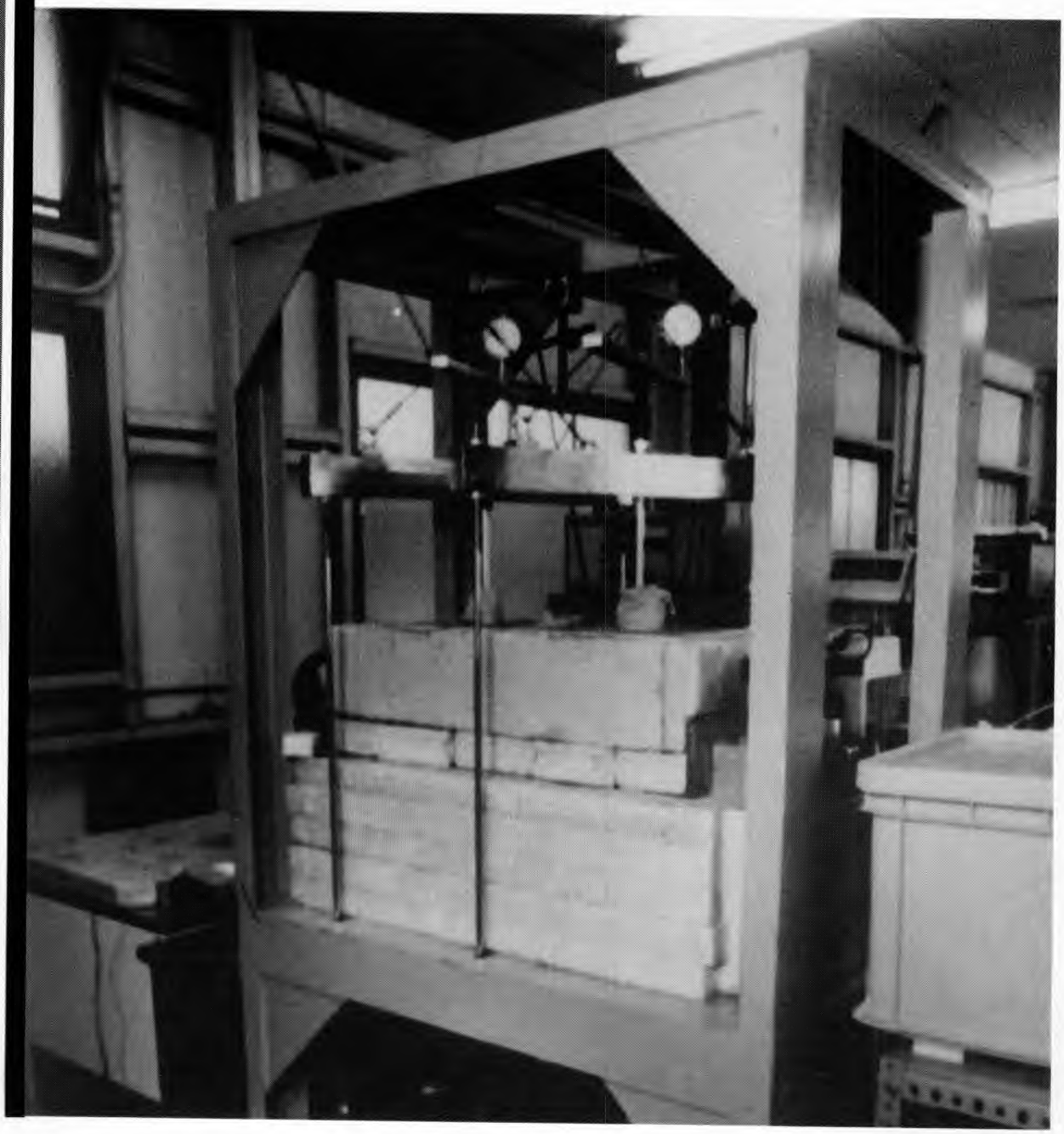

Abstract

A series of freezing tests on Kanto loam were conducted under various overburden pressures to find the steady growth condition of a segregated ice layer. The steady growth condition was found to be determined by the absolute value of the temperature gradient of the unfrozen part of the soil α_u near the 0°C isotherm and that of the frozen part of the soil α_f near the warmest end of an ice layer under given hydraulic conditions and applied effective pressure σ as follows: $\alpha_u = A\alpha_f$, $k_1/k_0 > A > S(\sigma)$; where k_1 and k_0 are the thermal conductivities of the frozen and unfrozen parts, respectively, A is a constant and S is an increasing function of σ. This is the first of a two-part presentation on the subject; the analytical aspects of the study are presented in a second report.

Cover: Apparatus for testing ice growth in soils under applied loads. (Photo by K. Takeda.)

For conversion of SI metric units to U.S./British customary units of measurement consult *Standard Practice for Use of the International System of Units (SI)*, ASTM Standard E380-89a, published by the American Society for Testing and Materials, 1916 Race St., Philadelphia, Pa. 19103.

CRREL Report 93-21

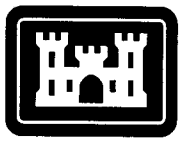

US Army Corps of Engineers
Cold Regions Research & Engineering Laboratory

Growth Condition of an Ice Layer in Freezing Soils Under Applied Loads

I. Experiment

Kazuo Takeda and Yoshisuke Nakano

November 1993

Prepared for
OFFICE OF THE CHIEF OF ENGINEERS

PREFACE

This report was prepared by Dr. Kazuo Takeda of the Technical Research Institute, Konoike Construction Co., Ltd., Konohana, Osaka, Japan, and Dr. Yoshisuke Nakano, Chemical Engineer, Applied Research Branch, Experimental Engineering Division, U. S. Army Cold Regions Research and Engineering Laboratory. Funding for this research was provided by DA Project 4A161102AT24, *Research in Snow, Ice and Frozen Ground*, Task SC, Work Unit F01, *Physical Processes in Frozen Soil.*

The authors thank Dr. V.J. Lunardini and Dr. Y.C. Yen of CRREL for technical review of this report.

CONTENTS

ILLUSTRATIONS

Figure

TABLES

Table

NOMENCLATURE

a_i	constant defined by eq 3 where $i = 0, 1$
A	constant
A_i	constant where $i = 0, 1$
d_i	density of the ith constituent
e	void ratio
f_i	mass flux of the ith constituent relative to that of soil minerals where $i = 1, 2$
f_{10}	mass flux of water in the unfrozen part of the soil
h	amount of heave
k_o	thermal conductivity of the unfrozen part of the soil
k_1	thermal conductivity of an ice layer
K_i	empirical function defined by eq 8a where $i = 1, 2$
K_{i1}	limiting value of K_i as x approaches n_1 while x is in R_1, $i = 1,2$
L	latent heat of fusion of water, 334 J g^{-1}
m	location of the top end of the specimen
M_i	name of a model where $i = 1, 2, 3$
n	boundary in R_o where the pressure of water is specified
n_i	boundary with $i = 0, 1$ where n_0 denotes the boundary where $T = 0°C$ and n_1 the interface between an ice layer and a frozen fringe
P_i	pressure of the ith constituent where $i = 1, 2$
P_{10}	value of P_1 at n_o
P_{21}	value of P_2 at n_1
r	rate of frost heave
R_o	unfrozen part of the soil
R_1	frozen fringe
R_2	ice layer
R_m	region in the diagram of temperature gradients where an ice layer melts
R_s	region in the diagram of temperature gradients where the steady growth of an ice layer occurs
R_s^*	boundary between R_s and R_u
R_s^{**}	boundary between R_m and R_s
R_u	region in the diagram of temperature gradients where the steady growth of an ice layer does not occur
S	defined by eq 10
S_o	value of S when $\sigma = 0$

SP_o	defined by eq 2
t	time
T	temperature
T_1	temperature at n_1
T_1^{**}	temperature at n_1 when eq 1 holds true
T_c	temperature of the cold bath
T_w	temperature of the warm bath
x	spatial coordinate
α_o	absolute value of the temperature gradient at n_o
α_1	absolute value of the limiting temperature gradient as x approaches n_1 while x is in R_2, defined by eq 5
α_f	absolute value of the temperature gradient near n_1 in R_2
α_u	absolute value of the temperature gradient near n_0 in R_0
γ	constant, 1.12 MPa °C^{-1}
σ	effective pressure defined by eq 1
i	subscript denotes the ith constituent of the mixture consisting of unfrozen water ($i = 1$), ice ($i = 2$) and soil minerals ($i = 3$)
*	superscript used to indicate the value of any variable evaluated when a point (α_1, α_0) in the diagram of temperature gradients is on R_s^*
**	superscript used to indicate the value of any variable evaluated when a point (α_1, α_0) in the diagram of temperature gradients is on R_s^{**}

Growth Condition of an Ice Layer in Freezing Soils Under Applied Loads

I. Experiment

KAZUO TAKEDA AND YOSHISUKE NAKANO

INTRODUCTION

When moist fine-grained soil freezes, it often is accompanied by volume expansion caused by the appearance of layers of more or less pure segregated ice within the soil. The scientific investigation of segregated ice began in the early 1900s, but the understanding gained by Taber (1929, 1930), Beskow (1935) and others, although useful, was largely qualitative. Since then a significant amount of effort has been made to gain a quantitative understanding on ice segregation.

We will consider the one-directional steady growth of an ice layer. Let the freezing process advance from the top down and the coordinate x be positive upwards with its origin fixed at some point in the unfrozen part of the soil. A transitional zone, often referred to as the frozen fringe, exists between the frost front (0°C isotherm) and the growing surface of an ice layer, though the nature of this zone has not been well understood. A freezing soil in this problem may be considered to consist of three parts: the unfrozen part R_0, the frozen fringe R_1 and the ice layer R_2, as shown in Figure 1.

Radd and Oertle (1973) studied the relationship between the pressure P_{21} and the temperature T_1 of an ice layer at n_1 by using a water-permeable, constant-volume cell in which the unfrozen part of a soil column was connected with a water reservoir subjected to an atmospheric pressure, $P_1 = 0.1$ (MPa). They found that there is a unique temperature T_1^{**} for given P_{21} and P_1 when an existing ice layer neither grows nor melts and the flux of water f_1 vanishes, and that T_1^{**} is given as:

$$\sigma = P_{21} - P_1 = -\gamma T_1^{**}, \qquad \text{if } f_1 = 0 \qquad (1)$$

where σ and P_{21} are often referred to as the effective pressure and the overburden pressure, respectively, and γ is a constant with the value of 1.12 MPa °C^{-1}. Equation 1 is often called the generalized Clausius-Clapeyron equation, which is attributed to Edlefsen and Anderson (1943). Studying the relationship between the effective pressure σ and T_1^{**} by using a closed constant-volume cell, Takashi et al. (1981) confirmed the validity of eq 1.

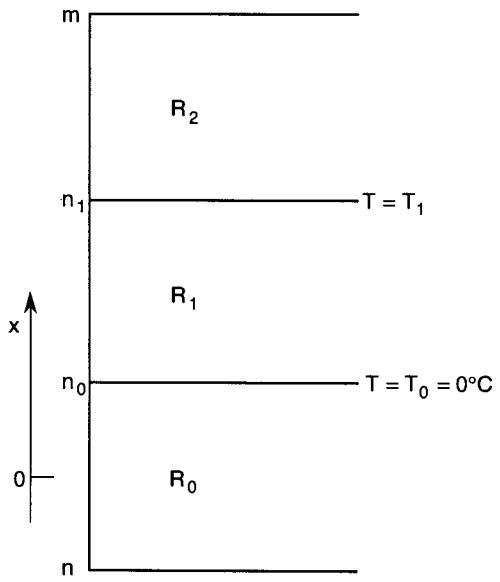

Figure 1. A steadily growing ice layer in a freezing soil.

Konrad and Morgenstern (1980, 1981, 1982) empirically found that the rate of water intake, f_{10}, at the formation of the final ice lens is proportional to the average temperature gradient $(T')_a$ in the frozen fringe when a soil sample freezes under different cold-side step temperatures but the same warm-side temperature under atmospheric conditions. This may be written as:

$$f_{10} = -SP_0(T')_a \tag{2}$$

where a prime denotes differentiation with respect to x. The positive proportionality factor SP_0 was found to be constant for a given soil and was termed the segregation potential. They also found empirically that SP_0 depends on the pressure of water P_{10} at n_0 and the applied pressure σ.

Studying the relationship between f_{10} and $(T')_a$ experimentally, Ishizaki and Nishio (1985) confirmed the validity of eq 2 at the formation of the final ice lens. They also found that f_{10} is a linear function of the temperature difference, $\Delta T = T_1^{**} - T_1$, during the stable growth period of the final ice lens, namely:

$$\Delta T = a_0 + a_1 f_{10} \tag{3}$$

$$\Delta T = T_1^{**} - T_1 \tag{4}$$

where a_0 and a_1 are constants. Nakano and Takeda (1991) confirmed empirically the validity of eq 3 when $\sigma = 0$.

We studied mathematically and experimentally the steady growth condition of an ice layer under negligible applied pressure in three earlier reports in this series (Nakano 1990, Takeda and Nakano 1990, Nakano and Takeda 1991). We have shown that for a given hydraulic condition the steady growth condition is determined by the absolute value of the temperature gradient α_0 at n_0 and the limiting value of the temperature gradient α_1 in R_2 defined as:

$$\alpha_1 = -\lim_{\substack{x \to n_1 \\ x \text{ in } R_2}} T'(x). \tag{5}$$

The steady growth condition is presented in the diagram of temperature gradients as shown in Figure 2. The steady growth occurs in the region R_s bounded by R_s^{**} and R_s^*. The boundary R_s^{**} is a straight line given as

$$\alpha_0 = (k_1/k_0)\,\alpha_1 \tag{6}$$

where k_1 and k_0 are the thermal conductivities of R_2 and R_0, respectively. We will refer to the region as R_m where $\alpha_0 > (k_1/k_0)\alpha_1, f_{10} < 0$ and an ice layer is melting. It should be mentioned that an existing ice layer neither grows nor melts, f_{10} vanishes and eq 1 holds true on R_s^{**}.

The boundary R_s^* is approximately a straight line given as:

$$\alpha_0 = S_0\,\alpha_1 \quad k_1 k_0^{-1} > S_0 > 0 \tag{7}$$

where S_0 is a constant that depends on only the properties of a given soil if $\alpha_0 > 2.0$ (°C cm^{-1}). The steady growth of an ice layer does not occur in the region R_u where $\alpha_0 < S_0\alpha_1$.

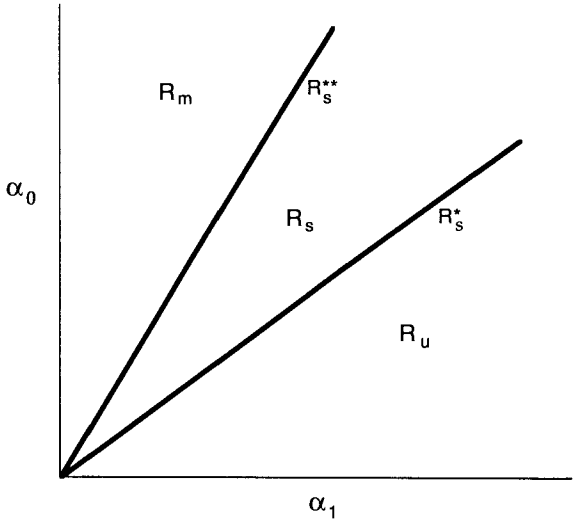

Figure 2. Temperature gradients α_1 and α_0.

We introduced a model M_1 (Nakano 1990) of a frozen fringe where ice may exist but does not grow, and the mass flux of water $f_1 (= f_{10})$ is given as

$$f_1 = -K_1 \frac{\partial P_1}{\partial x} - K_2 \frac{\partial T}{\partial x} \qquad \text{for } x \text{ in} R_1 \tag{8a}$$

$$K_2/K_1 \to \gamma \qquad \text{as} f_1 \to 0 \tag{8b}$$

$$\lim_{\substack{x \to n_1 \\ x \text{ in } R_1}} P_1(x) = P_2(n_1) = P_{21} \tag{8c}$$

where K_1 and K_2 are properties of a given soil that generally depend on T and the composition of the soil.

In the three earlier reports in this series we showed that M_1 is consistent with eq 1 (Nakano 1990), eq 3 and 7 under $\sigma = 0$ (Nakano and Takeda 1991). We also showed (Nakano and Takeda 1991) that the boundary R_s^* under $\sigma = 0$ is given as:

$$\alpha_0 = k_1 \left(k_0 + LbK_{21}^*\right)^{-1} \alpha_1 \tag{9}$$

where L is the latent heat of fusion of water, b is a function of the thickness δ of R_1 defined by eq 73c and 73e in Nakano (1990), and K_{21} is the limiting value of K_2 as x approaches n_1 while x is in R_1. An asterisk denotes that K_{21}^* is the value of K_{21} when a point (α_1, α_0) is on R_s^* in the diagram of temperature gradients.

This is the first of a two-part presentation on the effects of applied pressure on the steady growth condition of an ice layer. The objective of this work is to show empirically how the applied pressure affects the steady growth condition of an ice layer. In the following work we will show that the model M_1 is consistent with experimental data presented in this work. Moreover, we will show that M_1 is consistent with the reported empirical relationships, such as eq 2 and 3, under applied pressure.

EXPERIMENT

The same test apparatus used in the previous study (Takeda and Nakano 1990) was combined with a loading device that imposed a specified effective pressure σ on a test specimen as shown in Figure 3a. Since the weight of this loading device is balanced by the counterweight, only a specified and constant pressure σ is applied on the moving top surface of the specimen, provided that the friction of the suspending wire for the counterweight is negligibly small. However, the friction of the wire is not negligible when σ is small. Therefore, a weight was applied directly on the top of the specimen when σ was less than 50 kPa. Figure 3b is a photograph of the test apparatus.

A schematic drawing of the test cell is shown in Figure 3c. The test cell used in this study is essentially the same as that used in Takeda and Nakano (1990) except for minor modifications described below. In order to improve the accuracy of temperature measurements, one more thermocouple was added at $x = -1.0$ cm in the center of the unfrozen part of the specimen where a one-dimensional coordinate x is introduced with its origin at the level of the water reservoir, as shown in Figure 3a. Hence, four thermocouples were placed at $x = 0.0, -0.5, -1.0$ and -1.8 cm in the center of the specimen and four thermocouples at $x = 0.0$, 0.5, 1.0 and 1.8 cm along the inside wall of the sample holder. In order to suppress the heat transport through the loading arm, a plastic disk was placed on the top of an aluminum disk. The diameter of these two disks was slightly less than the inner diameter of the test cell so that the disks smoothly slided upward during the test.

In Figure 3a only one soil specimen is shown. However, in all freezing tests two duplicated soil specimens were tested simultaneously under the same condition to confirm the reproducibility of

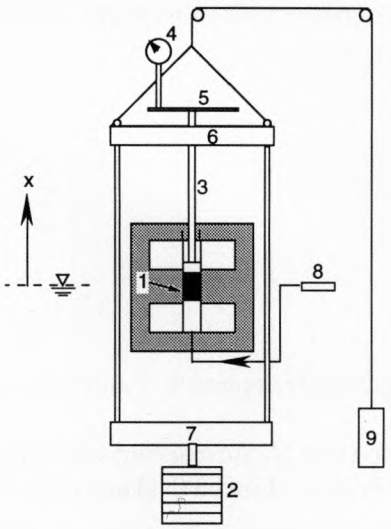

a. Schematic of test apparatus.

1. Soil specimen.
2. Load.
3. Loading arm.
4. Dial gauge.
5. Offset bar.
6. Upper load-guide bar.
7. Lower load-guide bar.
8. Water reservoir.
9. Counterweight.

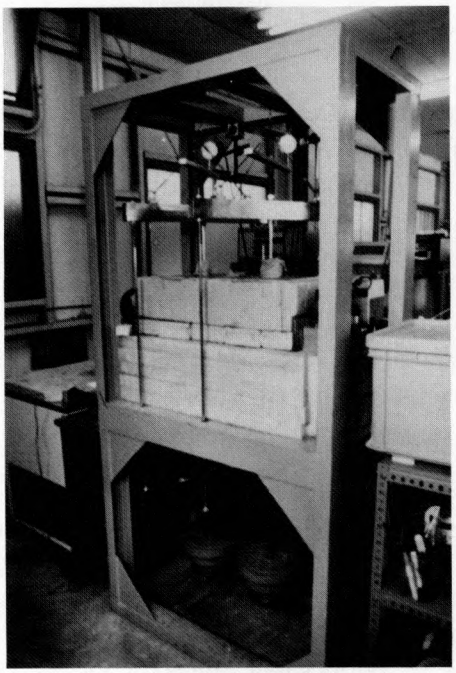

b. Test apparatus.

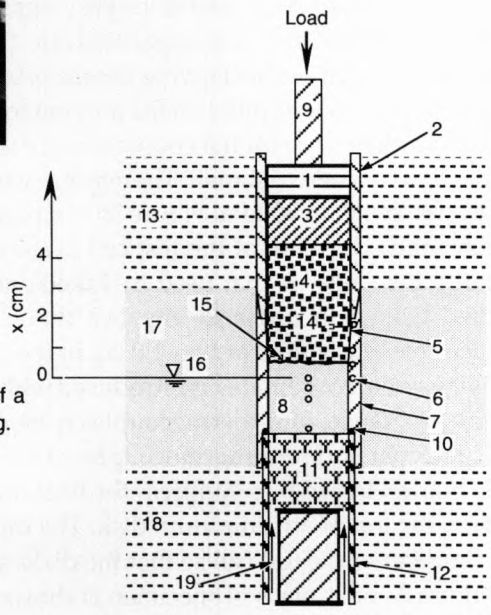

c. Schematic of test cell.

1. Plastic disk.
2. Upper cylinder.
3. Aluminum disk.
4. Frozen soil.
5. Teflon tape.
6. Thermocouple.
7. Sample holder.
8. Unfrozen soil.
9. Loading arm.
10. O-ring.
11. Glass beads.
12. Lower cylinder.
13. Cold bath.
14. Position of the top surface of a soil specimen before freezing.
15. Freezing front.
16. Initial water head.
17. Thermal insulator.
18. Warm bath.
19. Direction of water flow.

Figure 3. Test apparatus and test cell.

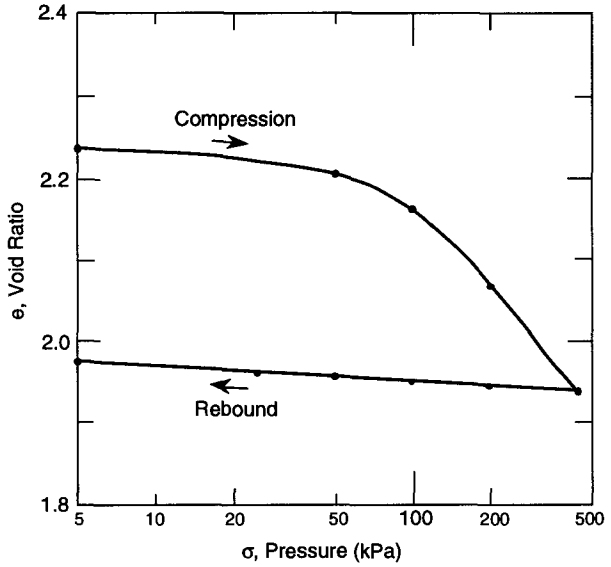

Figure 4. Consolidation characteristics (e vs. σ kPa) of Kanto loam.

test results. Kanto loam was used as a soil specimen. The properties of this soil were described in the previous paper (Takeda and Nakano 1990). A sample soil was mixed with water to make a de-aired slurry. The slurry was placed in a sample holder and was consolidated in steps to a final pressure 400 kPa in 10 days. Then the consolidated specimen was kept under a given test pressure σ ($\leq$ 390 kPa) for more than 48 hours to become equilibrated.

The data on the relationship between the void ratio e and the applied pressure σ in the rebound process are presented in Figure 4. From the data we find that the variation of e in the whole range of $\sigma < 400$ kPa amounts to 2% at most. Although the variation of e itself is negligibly small, some of physical properties such as the hydraulic conductivity may be affected significantly by such a small variation. We will further discuss the effects of e in the following report.

The temperature T_c of the cold bath and the temperature T_w of the warm bath were kept constant at specified values for more than 12 hours so that the temperature profile in the specimen would reach a thermal equilibrium. The specified values of T_c were between 0°C and –2°C. The freezing test began with the ice nucleation induced by putting a very small piece of ice on the top surface of the specimen.

At the beginning of the test the freezing front n_1 rapidly penetrated into the specimen. By changing the temperatures T_c and/or T_w in steps, we could stop the freezing front n_1 in a specified region, $0 < x < 1.0$ cm. We let an ice layer grow in the specified region for two reasons. First, one of four thermocouples for measuring temperatures in the unfrozen part of the specimen was located at $x = 0.0$ cm. Secondly, the hydraulic condition in our tests was specified by the distance δ_0 between n_0 and n, where n is defined as the interface between the glass beads and the specimen and the pressure of water was kept at the atmospheric pressure. Therefore, it was important to conduct all tests under nearly the same hydraulic conditions. Since n_1 was intentionally positioned in the region specified above, the measurements of temperature in R_2 were made by the thermocouples along the inside wall of the sample holder. Although the differences between the measured temperature at the center of the specimen and that along the inside wall at $x = 0.0$ cm were found to be quite small, the temperature measurements in R_0 were more accurate than those in R_2 because the temperature at the center was closer to the average temperature over the cross section of the specimen.

As soon as the freezing front stopped and the thermal field in the specimen attained a steady condition, an ice layer emerged (initiation of ice segregation). From the measured temperature profile we calculated a pair of variables (α_f^*, α_u^*) where the asterisks denote the values of a pair (α_f, α_u) at the initiation of ice segregation. As we will show below, the measured temperature profiles in R_0 (or R_2) were nearly linear when the steady growth of an ice layer took place. The value of α_u (or α_f) was calculated for the most part from the measured temperatures at the two points nearest to n_0 (or n_1) in R_0 (or R_2).

As discussed in Nakano and Takeda (1991), the amount of heat transported by convection is much less than that transported by conduction in our experiments and, as the result, the temperature profiles in R_0 (or R_2) become nearly linear. After obtaining the first pair, we changed T_c and/or T_w such that the freezing front moved a little and a new ice layer emerged at a new site slightly below the previous site. Repeating the same procedure, we obtained several pairs of (α_f^*, α_u^*) in the specified region described above. A series of tests were conducted under various applied pressures. The test conditions of all tests are summarized in Table 1.

Table 1. Test conditions.

σ (kPa)	No. of runs	T_c (°C)	T_w (°C)	No. of pairs (α_f^*, α_u^*)
0.0	14	−6.1 to −20.0	5.3 to 19.6	14
8.1	4	−3.3 to −14.9	3.0 to 15.1	5
16.2	3	−1.6 to −14.3	1.6 to 14.0	8
48.7	3	−1.3 to −13.5	1.6 to 13.0	6
97.5	2	−1.4 to −16.2	3.0 to 28.2	9
195	2	−1.3 to −17.1	2.0 to 32.2	9
390	2	−2.8 to −18.6	5.0 to 35.8	6

TEST RESULTS

Several variables were measured during the test. The temperature at the location of each thermocouple was measured at least twice every hour, while the amount of heave h and the location of the freezing front n_1 were measured at least once every hour. The amount of water taken away from the reservoir was measured at suitable intervals, depending upon the amount. The accuracy of these measurements was described in the previous study (Takeda and Nakano 1990).

We will show the behavior of measured variables with time by using the set of data obtained under the applied pressure of 195 kPa as an example. The records of T_c and T_w are shown in Figure 5a. Since T_c and T_w were changed stepwise, the records look like a step function. Despite the stepwise change of T_c and T_w, all other measured variables described above changed more or less continuously with respect to time. The amount of heave h and the position of n_1 are plotted vs. time in Figure 5b.

The rate of heave r was calculated from the measured $h(t)$ as the average over a finite time interval, while the rate of water intake f_{10} was calculated from the measured amount of water in the reservoir as the average over another finite time interval. The calculated values of r and f_{10} are plotted vs. time in Figure 5c where each horizontal line is the average over the time interval corre-

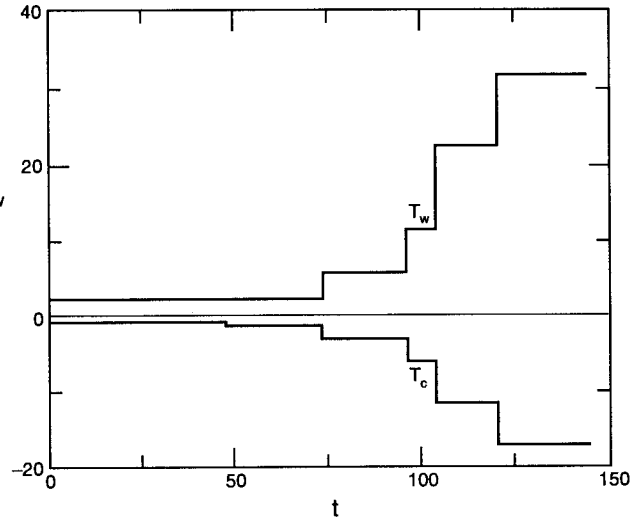

a. Temperatures T_c °C and T_w °C vs. t hours with σ = 195 kPa.

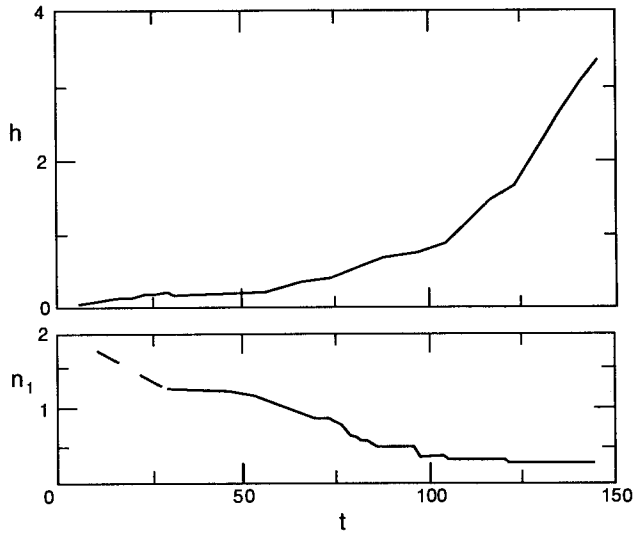

b. Measured h cm and n_1 cm vs. t hours with σ = 195 kPa.

Figure 5. Measured variables vs. time for σ = 195 kPa.

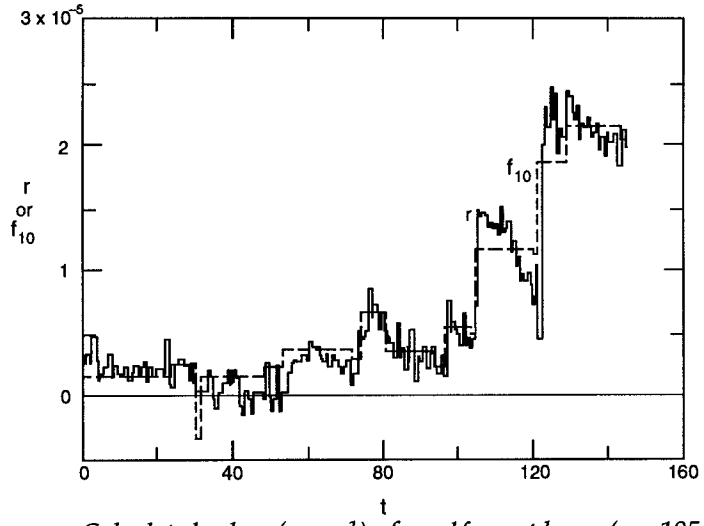

c. Calculated values (cm s^{-1}) of r *and* f_{10} *vs.* t *hours* ($\sigma = 195$ *kPa).*

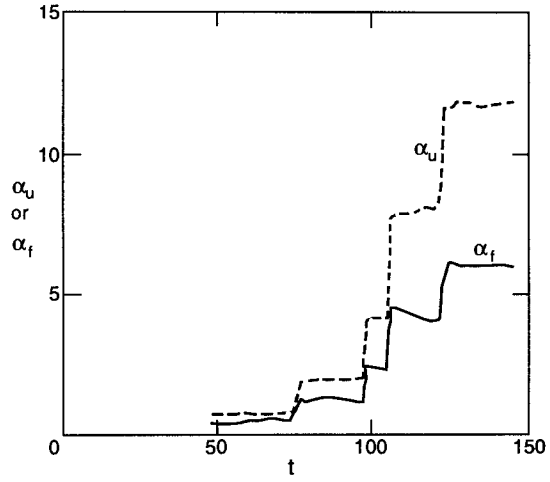

d. Calculated values (°C cm^{-1}) of α_f *and* α_u *vs.* t *hours* ($\sigma = 195$ *kPa).*

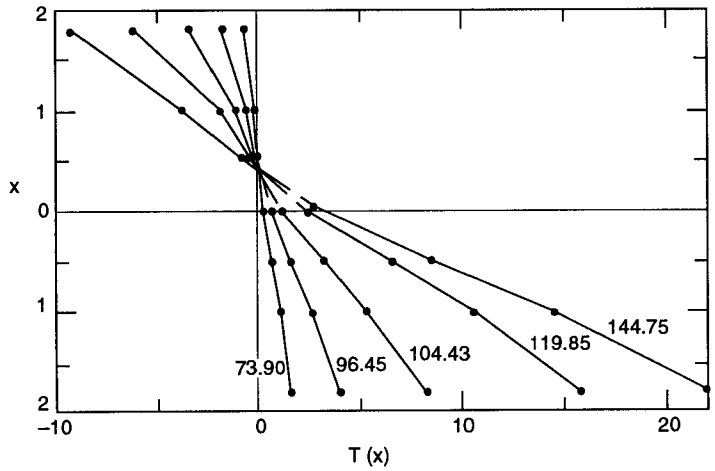

e. Measured temperature profiles T(x)°C *in the specimen at* t = *73.90, 96.45, 104.43, 119.85 and 144.75 hours* ($\sigma = 195$ *kPa).*

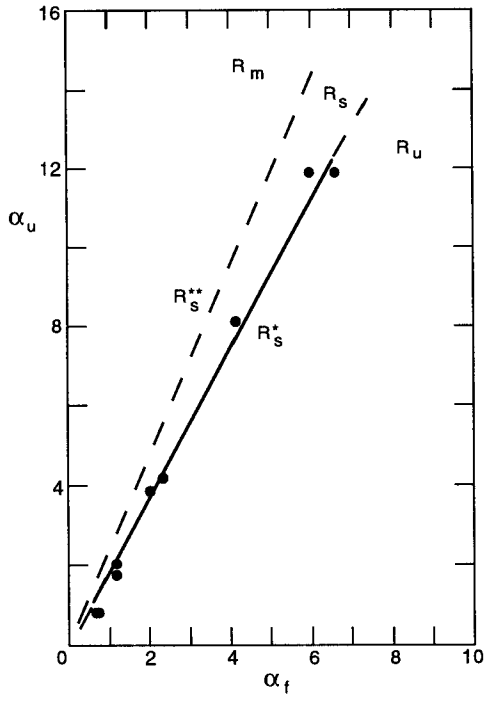

f. Steady growth region R_s ($\sigma = 195$ *kPa).*

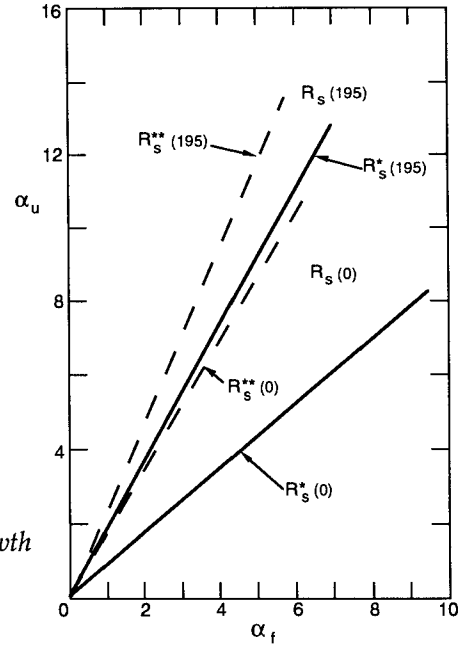

g. Steady growth region $R_s(\sigma)$.

Figure 5 (cont'd).

sponding to the line length. Similarly, the calculated average values of α_f and α_u from the measured temperature profiles over certain variable intervals are plotted vs. t in Figure 5d.

The measured temperature profiles in the specimen at 73.90, 96.45, 104.43, 119.85 and 144.75 hours are presented in Figure 5e, where dark circles are data points and straight lines are drawn between two neighboring points. It is easy to see from Figure 5e that each solid line in the frozen or the unfrozen part of the specimen is nearly linear. This implies that the thermal field was nearly steady at each of those points of time when the initiation of ice segregation occurred and a pair of (α_f^*, α_u^*) were obtained.

At the beginning of this test, T_c and T_w were kept constant at –0.9°C and 2.0°C, respectively. The freezing front n_1 moved downward rapidly. At 48.3 hours T_c was decreased to –1.3°C so that the penetrating speed of n_1 would be slowed while T_w was kept constant. At about 55.0 hours the speed of n_1 increased again and the rate of heave r began increasing to attain a maximum at 61.0 hours. After 61.0 hours r decreased and n_1 gradually approached $x = 0.85$ cm. At 71.4 hours a segregated ice layer without any visible soil particles emerged as soon as n_1 ceased to move. At this time r became nearly constant and the values of α_f and α_u remained constant. Under such a steady condition, the ice layer kept growing while n_1 remained still until 73.9 hours. We found these constant values of α_f and α_u to be α_f^* and α_u^*, respectively. In other words, a constant pair (α_f^*, α_u^*) was on R_s^*.

After obtaining the first pair (α_f^*, α_u^*), we changed T_c and T_w in such a manner that n_1 moved downward slightly and a new ice layer emerged at a new location slightly below the previous ice layer. Repeating the same procedure, we obtained several pairs of (α_f^*, α_u^*). As shown in Figure 5d, it took a few hours for α_f and α_u to stabilize after T_c and / or T_w were changed stepwise. It is clear from Figures 5c and 5d that the values of r and f_{10} were sensitively affected by minor variations of α_f and α_u. When r is quite small, accurate measurement of the rate of water intake over a short time interval was difficult. Therefore, the mass flux of water was usually calculated based on r under such a case.

From two tests under the condition of σ = 195 kPa, we obtained nine pairs of (α_f^*, α_u^*) that are plotted in the diagram of temperature gradients in Figure 5f. As in the previous study (Takeda and Nakano 1990), we will seek a linear approximation to the relation between α_f^* and α_u^* given as:

$$\alpha_u^* = S(\sigma)\,\alpha_f^* \tag{10}$$

where the positive proportionality factor S is assumed to depend on only the applied pressure σ. Using the method of interval estimate (Fisz 1965), we have found from the data set that the value of $S(195)$ is 1.856. The line $R_s^*(195)$ passing through the data points in Figure 5f is given by eq 10 with σ = 195 kPa, which is a linear approximation to the boundary R_s^* that divides the steady growth region R_s and the region R_u where the steady growth of an ice layer does not occur.

The broken line R_s^{**} (195) in Figure 5f is given as:

$$\alpha_u = [k_1(\sigma)/k_0]\alpha_f\,, \qquad \sigma = 195 \text{ kPa}. \tag{11}$$

We found empirically that the thermal conductivity k_0 of the unfrozen part of a specimen is hardly affected by the applied pressure σ. However, σ affects the thermal conductivity k_1 of an ice layer to a degree that is minor but not negligible. The measured average densities d_2 and conductivities k_1 of ice layers under various σ values are presented in Table 2. It is easy to see that the values of d_2 when $\sigma > 0$ are greater than when $\sigma = 0$. The applied pressure evidently reduces the amount of space occupied by air in ice layers and, as a result, the values of k_1 when $\sigma > 0$ are also greater than when $\sigma = 0$ as shown in Table 2.

Table 2. Summary of test results.

σ (kPa)	$S(\sigma)$	d_2 (g cm^{-3})	k_1 J (cm s °C)$^{-1}$	$k_1 k_0^{-1}$*
0.0	0.871	0.860	1.59E-2†	1.73
8.1	1.078	0.898	2.13E-2	2.31
16.2	1.554	0.895	2.12E-2	2.30
48.7	1.618	0.907	2.19E-2	2.38
97.5	1.817	0.906	2.18E-2	2.37
195	1.856	0.907	2.19E-2	2.38
390	1.985	0.904	2.17E-2	2.36

* $k_0 = 9.20 \times 10^{-3}$ J/(cm s °C).
† $E - N = 10^{-N}$.

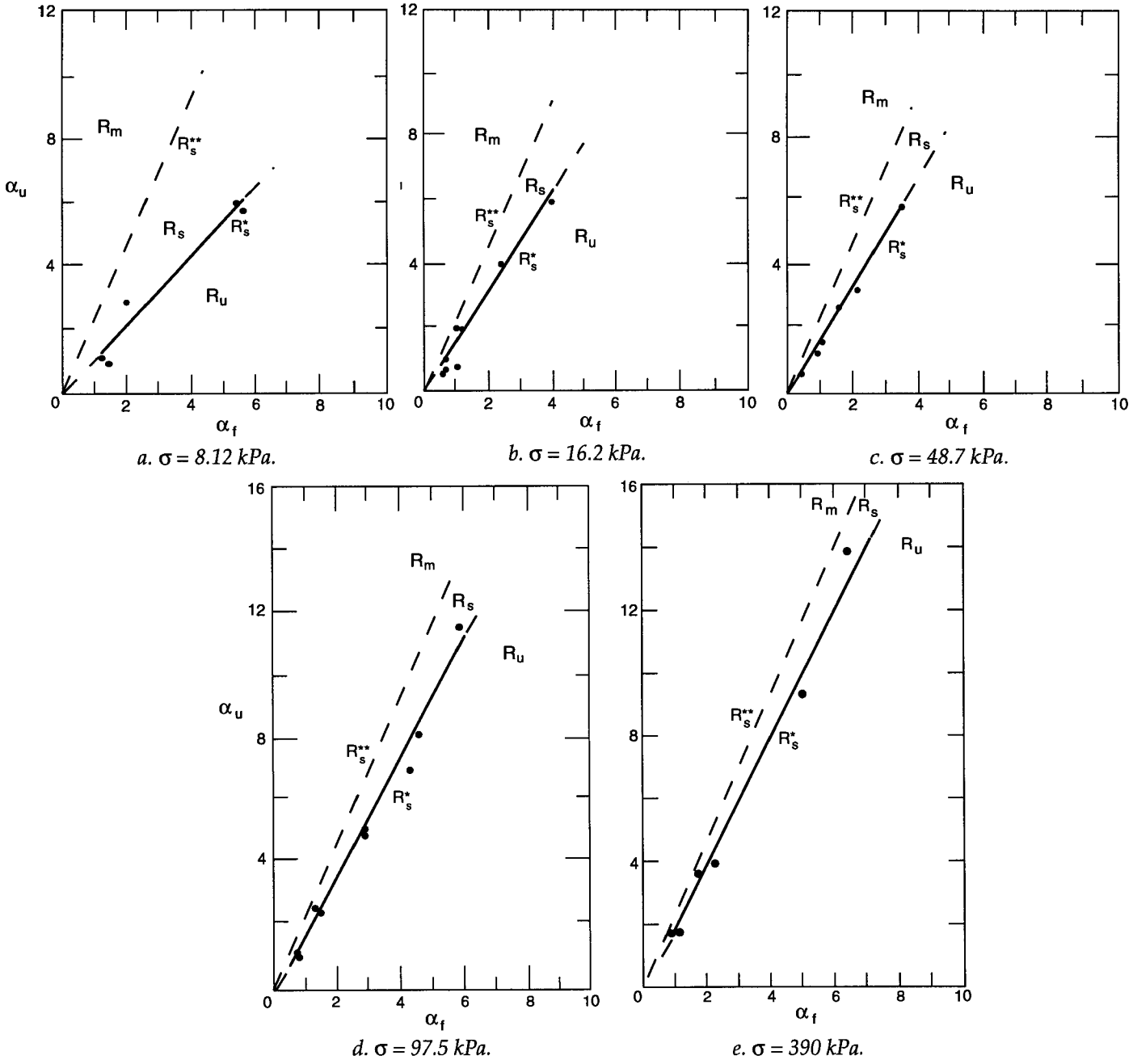

Figure 6. Steady growth region R_s.

The values of (k_1/k_0) with σ = 195 kPa and σ = 0.0 kPa are 2.38 and 1.73, respectively, as given in Table 2. Because of this difference the broken line R_s^{**} (0) given by eq 11 with σ = 0.0 lies below the line R_s^{**} (195) as shown in Figure 5g. The steady growth region R_s(195) under σ = 195 kPa is the region bounded by R_s^* (195) and R_s^{**} (195) while that under σ = 0.0 kPa is the region bounded by R_s^* (0) and R_s^{**} (0) in Figure 5g. It is clear from this figure that the applied pressure of 195 kPa significantly reduced the area of the steady growth region.

Using the same test procedure as described above for the case of σ = 195 kPa, we conducted a series of tests under various applied pressures to determine the region of steady growth $R_s(\sigma)$ for a given σ. The results of these tests are presented in Figure 6a (σ = 8.12 kPa), 6b (16.2 kPa), 6c (48.7 kPa), 6d (97.5 kPa) and 6e (390 kPa). It is clear from Figures 5g and 6 that the region of steady growth $R_s(\sigma)$

tends to decrease with increasing σ. The values of $S(\sigma)$ given in Table 2 are plotted vs. σ in Figure 7. It is found from Figure 7 that the value of S increases sharply with increasing σ when σ is small and that the rate of increase slows down as σ becomes greater. A curve in Figure 7 is one example of the approximate presentation of data points given as

$$S(\sigma) = 0.280\ \sigma^{0.243} + 0.856 \qquad (12)$$

where σ is in kilopascals.

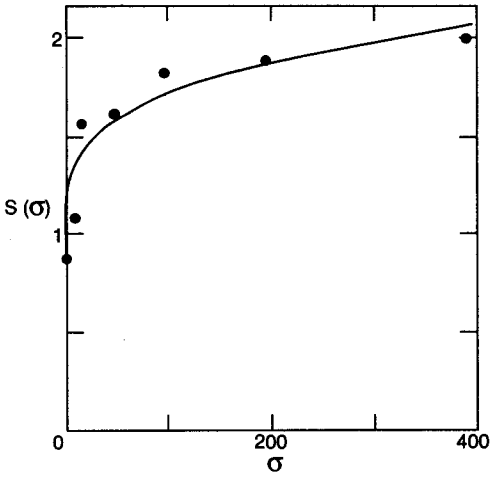

Figure 7. Values of S(σ) *vs.* σ *(kPa).*

We have found empirically (Takeda and Nakano 1990) that there is the upper bound A_1 (or A_0) of α_f (or α_u) beyond which an ice layer with cavities grows when σ is negligibly small and that the value of A_1 for Kanto loam is 8.8°C cm^{-1}. The reason for such behavior was explained (Takeda and Nakano 1990, Nakano and Takeda 1991) as follows. The pressure P_{10} of water at n_0 decreases with the increasing value of α_f (or f_{10}) until P_{10} attains a value that corresponds to the air entry value of Kanto loam when an ice layer with cavities begins growing. The growth of an ice layer with cavities was not observed in all the tests under various applied pressures presented in this work. Consequently, we were unable to confirm the upper bound of α_f in this work.

CONCLUSIONS

A series of freezing tests on Kanto loam were conducted under various overburden pressures to find the steady growth condition of a segregated ice layer. The steady growth condition was found to be determined by the absolute value of the temperature gradient of the unfrozen part of the soil α_u near the 0°C isotherm and that of the frozen part of the soil α_f near the warmest end of an ice layer under given hydraulic condition and applied effective pressure as follows:

$$\alpha_u = A\alpha_f, \qquad k_1/k_0 > A > S(\sigma) \qquad (13)$$

where $S(\sigma)$ is an increasing function of σ.

This is the first of a two-part presentation on the effects of applied pressure on the steady growth condition of an ice layer. In the following paper we will show that the model M_1 is consistent with experimental data presented in this work.

LITERATURE CITED

Beskow, G. (1935) Soil freezing and frost heaving with special attention to roads and railroads. *Swedish Geological Society Yearbook*, Series C, **26**(3): 1–145.

Edlefsen, N.W. and A.B.C. Anderson (1943) Thermodynamics of soil moisture. *Hilgardia*, **15**(2): 31–298.

Fisz, M. (1965) *Probability Theory and Mathematical Statistics.* New York: John Wiley & Sons, p. 461.

Ishizaki, T. and N. Nishio (1985) Experimental study of final ice lens growth in partially frozen saturated soil. In *Proceedings, 4th International Symposium on Ground Freezing, 5–7 August, Sapporo, Japan* (S. Kinoshita and M. Fukuda, Ed.). Rotterdam, Netherlands: A.A. Balkema, p. 71–78.

Konrad, J.M. and N.R. Morgenstern (1980) A mechanistic theory of ice lens formation in fine-grained soils. *Canadian Geotechnical Journal*, **17**: 473–486.

Konrad, J.M. and N.R. Morgenstern (1981) The segregation potential of a freezing soil. *Canadian Geotechnical Journal*, **18:** 482–491.
Konrad, J.M. and N.R. Morgenstern (1982) Effects of applied pressure on freezing soils. *Canadian Geotechnical Journal*, **19:** 494–505.
Nakano, Y. (1990) Quasi-steady problems in freezing soils: I. Analysis on the steady growth of an ice layer. *Cold Regions Science and Technology*, **17**(3): 207–226.
Nakano, Y. and K. Takeda (1991) Quasi-steady problems in freezing soils: III. Analysis on experimental data. *Cold Regions Science and Technology*, 19: 225–243.
Radd, F.J. and D.H. Oertle (1973) Experimental pressure studies of frost heave mechanism and the growth-fusion behavior of ice. In *Permafrost: The North American Contribution to the 2nd International Conference on Permafrost, Yakutsk, 13–28 July*. Washington, D.C.: National Academy of Sciences, p. 377–384.
Taber, S. (1929) Frost heaving. *Journal of Geology*, **37**(1): 428–461.
Taber, S. (1930) The mechanics of frost heaving. *Journal of Geology*, **38:** 303–317.
Takashi, T., T. Ohrai, H. Yamamoto and J. Okamoto (1981) Upper limit of heaving pressure derived by pore-water pressure measurements of partially frozen soil. *Engineering Geology*, **18:** 245-257.
Takeda, K. and Y. Nakano (1990) Quasi-steady problems in freezing soils: II. Experiment on steady growth of an ice layer. *Cold Regions Science and Technology*, **18:** 225-247.

REPORT DOCUMENTATION PAGE

Form Approved
OMB No. 0704-0188

1. AGENCY USE ONLY (Leave blank)	2. REPORT DATE	3. REPORT TYPE AND DATES COVERED
	November 1993	

4. TITLE AND SUBTITLE

Growth Condition of an Ice Layer in Freezing Soils Under Applied Loads: I. Experiment

5. FUNDING NUMBERS

PE: 6.11.02A
PR: 4A161102AT24
TA: SC
WU: F01

6. AUTHORS

Kazuo Takeda and Yoshisuke Nakano

7. PERFORMING ORGANIZATION NAME(S) AND ADDRESS(ES)

Konoike Construction Co., Ltd. and Konohana, Osaka, Japan

U.S. Army Cold Regions Research and Engineering Laboratory
72 Lyme Road
Hanover, New Hampshire 03755-1290

8. PERFORMING ORGANIZATION REPORT NUMBER

CRREL Report 93-21

9. SPONSORING/MONITORING AGENCY NAME(S) AND ADDRESS(ES)

Office of the Chief of Engineers
Washington, D.C. 20314-1000

10. SPONSORING/MONITORING AGENCY REPORT NUMBER

11. SUPPLEMENTARY NOTES

12a. DISTRIBUTION/AVAILABILITY STATEMENT

Approved for public release; distribution is unlimited.

Available from NTIS, Springfield, Virginia 22161.

12b. DISTRIBUTION CODE

13. ABSTRACT (*Maximum 200 words*)

A series of freezing tests on Kanto loam were conducted under various overburden pressures to find the steady growth condition of a segregated ice layer. The steady growth condition was found to be determined by the absolute value of the temperature gradient of the unfrozen part of the soil α_u near the 0°C isotherm and that of the frozen part of the soil α_f near the warmest end of an ice layer under given hydraulic conditions and applied effective pressure σ as follows: $\alpha_u = A\alpha_f$, $k_1/k_0 > A > S(\sigma)$; where k_1 and k_0 are the thermal conductivities of the frozen and unfrozen parts, respectively, A is a constant and S is an increasing function of σ. This is the first of a two-part presentation on the subject; the analytical aspects of the study are presented in a second report.

14. SUBJECT TERMS

Freezing fronts
Freshwater ice
Frozen soils
Ice lenses
Mathematical analysis

15. NUMBER OF PAGES
19

16. PRICE CODE

17. SECURITY CLASSIFICATION OF REPORT	18. SECURITY CLASSIFICATION OF THIS PAGE	19. SECURITY CLASSIFICATION OF ABSTRACT	20. LIMITATION OF ABSTRACT
UNCLASSIFIED	UNCLASSIFIED	UNCLASSIFIED	UL